Influence of bulk-phonon-branch dispersion on displacement patterns and the intermixing of interface and confined optical phonons in superlattices

H. Gerecke and F. Bechstedt
Friedrich-Schiller-Universität, Max-Wien-Platz 1, 6900 Jena, Germany
(Received 19 July 1990)

An envelope-function formalism is developed to treat zone-center superlattice phonons with inclusion of effects due to the full bulk-phonon-branch dispersion and the long-range macroscopic electric field. Starting from a rigid-ion model, differential equations for the envelopes of the atomic displacement patterns are derived. It is shown that both the transverse component of the electric field and the longitudinal component of the electric displacement field that appear automatically satisfy the boundary conditions of macroscopic electrodynamics. For optical and acoustical phonons, the same additional mechanical boundary conditions for the envelopes themselves are extracted from the underlying microscopic equations of motion. They therefore depend on the atomic structure of the interfaces. Explicit results are given for $(GaAs)_{N_1}(AlAs)_{N_2}$ (001) superlattices. In the case of *p*-polarized symmetrical modes they show a strong anisotropy and intermixing of nominal confined and interface optical phonons. The considered material combination with nearly the same bulk acoustic branches and well-separated optical-phonon bands allows some approximations giving physical insights into the correct solutions of the dispersionless macroscopic continuum theory. Starting from the concept of effective layer thicknesses or a band-edge expansion, one obtains analytical results for frequencies, confinement wave numbers, and displacement patterns, which represent generalizations of the macroscopic continuum theory with the influence of the bulk-phonon-branch dispersion taken into account.

I. INTRODUCTION

Raman scattering measurements have proved to be a powerful tool for studies of zone-center optical phonons and their interaction with electrons in superlattices. GaAs-$Ga_{1-x}Al_xAs$ superlattices have been among the most intensively studied systems in this respect.[1–14] Confined optical and interface phonons have been observed. Theoretical approaches of various complexity have been proposed[15–38] to explain the experimental findings. The conventional dielectric-continuum theory based on the Born-Huang equations and the neglect of the bulk-phonon-branch dispersion has been widely used in discussions of the occurrence and anisotropy of interface and confined slab modes, as well as their interaction with electrons or holes.[16,17,19–24] Microscopic calculations within the framework of the bond-charge model,[25] the shell model,[26] or rigid-ion models[27–30] have also been made.

The optical-phonon problem for superlattices formed by lattice-matched materials with nonoverlapping optical phonon branches may appear to be solved. However, as already noted by Sood *et al.*[3] the nodal structure and the symmetry of the atomic displacement patterns derived for long-wavelength bulklike confined modes within the conventional continuum model are at variance with those obtained from a certain microscopic calculation. They[3] and other authors[31] suggested that the application of the continuum theory and the boundary conditions of macroscopic electrodynamics to superlattices involving thin material layers and sharp interfaces extends the continuum theory beyond its legitimate limit. Starting from an idea of Klein[32] concerning the uncertainties in the solutions of the macroscopic theory working with dispersionless bulk-phonon branches, Huang and Zhu,[33] as well as the authors of the present paper,[34,35] reformulated the results of the macroscopic continuum model by a critical comparison of the macroscopic approach with a closely parallel microscopic model. These authors pointed out that the main failure of the continuum theory is due to the neglect of the bulk-phonon dispersion if appropriate solutions of the continuum approach are taken into account. Envelopes of the displacement patterns could be constructed which are in agreement with the microscopic theory; so a clear separation between bulklike confined and interface phonons is possible. Early attempts to include the dispersion of the bulk-phonon branches into the continuum theory have been made by several authors.[22,36–38] However, they are usually restricted to parabolic approximations of the bulk dispersion relations and incomplete solutions as far as the frequencies and displacement patterns are concerned.

In the present paper we develop a continuum theory for the vibronic problem of a superlattice, with inclusion of the full dispersion of the underlying bulk-optical-phonon branches. For clarity we restrict ourselves thereby to zone-center optical phonons of GaAs-AlAs (001) superlattices. Nevertheless, the results of the presented theory can be generalized to treat the phonon structure of similar superlattices as well. The paper is organized as follows. In Sec. II we present, in the framework of the continuum approach, equations of motion that are de-

rived from a microscopic force-constant model. The problem of mechanical and electric-field boundary conditions is discussed, starting from the same microscopic treatment. In Sec. III we write down the exact solutions for phonon frequencies and envelopes of the atomic displacements, even if some of the results are given only implicitly. In Sec. IV these results are extensively discussed and limiting cases are considered. We concentrate on the effects of the intermixing of nominal interface and bulk-like optical phonons due to the bulk-phonon-branch dispersion as well as on the dependence of the effective material-layer thicknesses on the specific dynamical matrix used. Finally, a summary is given.

II. ENVELOPE-FUNCTION THEORY

A. Equations of motion

Our starting point is a microscopic rigid-ion model introduced and discussed in detail in Refs. 30 and 34. The dynamical matrix is simplified in accordance with the common continuum theory.[15–17,19–24] More strictly, the elastic interactions between the atoms are restricted to first nearest neighbors and described by one radial force constant f_ℓ for each material. The coupling to the dipole-induced electric field is characterized by effective ion charges $\pm e^*$ for the cation (+) and anion (−). The value e^* is defined as Born's ion charge of the underlying zinc-blende-structure materials screened by the corresponding high-frequency electronic dielectric constant and assumed to be equal in both materials to avoid the charging effects of the interfaces. The electric field itself is spatially averaged over the Wigner-Seitz cell of the fcc structure underlying the superlattice materials.

As a prototype for the superlattices under consideration we discuss a $(\mathrm{GaAs})_{N_1}(\mathrm{AlAs})_{N_2}$ superlattice formed by lattice-matched zinc-blende-structure semiconductors and grown in the [001] direction. In terms of the common lattice constant a_0 the layer thickness of the two materials, GaAs ($\ell=1$) or AlAs ($\ell=2$), is defined by $d_\ell = N_\ell a_0/2$. The superlattice period is given by $d = d_1 + d_2 = (N_1+N_2)a_0/2$. Such a superlattice represents a tetragonal crystal with $2(N_1+N_2)$ atoms per elementary cell. Therefore we expect the appearance of $6(N_1+N_2)$ phonon branches j. Each branch exhibits a dispersion with the phonon wave vector $\mathbf{Q}$ from the first Brillouin zone of the superlattice. To simplify the vibronic problem we only consider phonons with vanishing wave vector propagating in a certain direction $\mathbf{e}_Q = \sin\theta\,\mathbf{e}_y + \cos\theta\,\mathbf{e}_z$, where θ is the angle between $\mathbf{e}_Q$ and the superlattice axis $\mathbf{e}_z$. The atoms within a superlattice elementary cell can be classified by the triple α,ℓ,c, where, besides the material index $\ell=1$ and 2, the atom index $\alpha=1$ ($\alpha=2$) characterizing the cation (anion) appears. The third number c is a molecular-layer (parallel to the interfaces) index, i.e., $1\le c\le N$, for GaAs and $N_1+1\le c\le N_1+N_2$ for AlAs.

To solve the vibronic problem characterized above, instead of the discrete (integer) index c in the microscopic theory we introduce a continuous variable z ($0\le z<d$) to describe the positions of the cations ($\alpha=1$) and anions ($\alpha=2$) within the superlattice elementary cell. Thereby the envelope functions $u_{\alpha\ell j\alpha}(z,\theta)$ of the Cartesian components ($\alpha=x,y,z$) of the atomic displacements resulting within our continuum theory must agree with atomic displacements $u_{\alpha\ell cj\alpha}(\theta)$ of the microscopic theory just at the discrete atomic positions $z=[2(c-1)+\delta_{\alpha 1}]a_0/4$. If one additionally assumes that all derivatives of the envelope functions with respect to z exist within each material layer, the equations of motion of an atom with the mass $M_{\alpha\ell}$ and the effective ion charge $\pm e^*$ can be written in the form ($\alpha,\alpha'=1,2;\alpha\neq\alpha'$)

$$[M_{\alpha\ell}\omega_j^2(\theta)-(f_\ell+\hat{f}\delta_{\alpha z})]u_{\alpha\ell j\alpha}(z,\theta)+(f_\ell+\hat{f}\delta_{\alpha z})\cosh\left[\frac{a_0}{4}\frac{d}{dz}\right]u_{\alpha'\ell j\alpha}(z,\theta)=(-1)^\alpha e^*[E_{jy}(\theta)\delta_{\alpha y}+D_{jz}(\theta)\delta_{\alpha z}]\,, \tag{1}$$

with the eigenfrequency $\omega_j(\theta)$ of a long-wavelength phonon from branch j and propagating in a certain direction θ. In Eq. (1) the Coulomb force constant $\hat{f}=16\pi(e^*)^2/a_0^3$ of the underlying polar bulk materials is introduced. It is responsible for the LO-TO splitting in the center of the Brillouin zone. The differential operator $\cosh(\frac{1}{4}a_0\,d/dz)$ is defined by the corresponding Taylor expansion. This particular form results from the representation of the displacements at $z\pm a_0/4$ by those at z. Its appearance is related to the fact that the bulk-phonon-branch dispersion is taken into account, at least in the framework of the simplified dynamical matrix used in this work. Neglecting the branch dispersion by taking the limit $a_0\to 0$, the difference of Eqs. (1) for cation and anion changes over in the known equation for the relative displacement of macroscopic theory.[34,35]

The driving forces on the right-hand side of Eq. (1) are related to the y component, $E_{jy}(\theta)$, of the spatially averaged electric field and to the z component, $D_{jz}(\theta)$, of the macroscopic dielectric displacement field. They are correctly defined by

$$e^*\begin{bmatrix}E_{jy}(\theta)\\ D_{jz}(\theta)\end{bmatrix}=-\hat{f}\sin\theta\begin{bmatrix}\sin\theta & \cos\theta\\ \cos\theta & -\sin\theta\end{bmatrix}\sum_{\alpha,\ell=1}^{2}\sum_{\substack{z\\(\text{atomic positions})}}\frac{(-1)^{\alpha-1}}{N_1+N_2}\begin{bmatrix}u_{\alpha\ell jy}(z,\theta)\\ u_{\alpha\ell jz}(z,\theta)\end{bmatrix}. \tag{2}$$

In the continuum limit $a_0 \to 0$ the sum in Eq. (2) defining the y and z components of the total electric dipole moment of the superlattice elementary cell changes over into an integral. The field components $E_{jy}(\theta)$ and $D_{jz}(\theta)$ are strongly angle dependent. Hence the electric-field-induced forces can produce a strong anisotropy with θ in the lattice vibrations, at least for their y and z components, corresponding to the reduced symmetry of the superlattice.

B. Boundary conditions

To couple Eqs. (1), defined only within one material layer, across the interfaces one has to adapt envelope functions from different adjacent materials. The long-range electric-field components $E_{jy}(\theta)$ and $D_{jz}(\theta)$ given in Eq. (2) are independent of the atomic and material indices α and ℓ. They are constant with respect to the position z of cations and anions within the superlattice elementary cell. Therefore the boundary conditions of the macroscopic electrodynamics—continuity of the normal component of the displacement field as well as that of the tangential component of the electric field—are automatically satisfied at the GaAs-AlAs interfaces for phonons from the Brillouin-zone center. Hence, no information on the behavior of the envelopes of the atomic displacements can be derived from the electrodynamics by applying the fields in Eq. (2).

Connection rules for the envelopes and their derivatives, which are by all means necessary, since the full dispersion of the bulk phonon branches is taken into Eqs. (1), should be obtained starting from the envelopes themselves. Babiker[22] adapted the familiar hydrodynamic boundary conditions concerning the continuity of velocity and pressure at the interface.[39] Using a similar parabolic expansion of the bulk-phonon branches, Akera and Ando[38] pointed out that the connection rules from elasticity theory—the continuity of displacement and stress across the interface—are in general not applicable to optical-phonon modes. Rather, one has to take into account the actual atomic structure of the interface as well as the applied dynamical matrix. We follow this line[18] of derivation of the boundary conditions because it should give rise, more or less, to the same results as the microscopic theory.[30]

In the case of GaAs-AlAs superlattices, only one interface type appears. By reason of the actual symmetry, the interface at $z=0$ (or $z=d$) should be identified with the arsenic layer embedded between an Al layer on the left and a Ga layer on the right and vice versa for that at $z=d_1$. In the framework of the continuum approach and the equivalence of the two interfaces at $z=0$ (or $z=d$) and $z=d_1$ per superlattice elementary cell, a first boundary condition, the continuity of the anion envelope functions,

$$u_{21j\alpha}(z,\theta)|_{z=d_1-0}=u_{22j\alpha}(z,\theta)|_{z=d_1+0} , \tag{3}$$

follows automatically. A second condition results directly from the microscopic equation of motion for the anions. At the interfaces the cation envelope functions should be connected by

$$(f_1+\hat{f}\delta_{\alpha z})\sinh\left[\frac{a_0}{4}\frac{d}{dz}\right]u_{11j\alpha}(z,\theta)\Big|_{z=d_1-0}$$
$$=(f_2+\hat{f}\delta_{\alpha z})\sinh\left[\frac{a_0}{4}\frac{d}{dz}\right]u_{12j\alpha}(z,\theta)\Big|_{z=d_1+0} . \tag{4}$$

Neglecting the bulk-phonon-branch dispersion, i.e., considering the limit $a_0 \to 0$, relation (4) gives rise to a connection rule for the first derivatives of the cation displacements.

As a consequence of expressions (3) and (4) it is in general problematical to derive defined boundary conditions for the envelope function of the relative displacements of the cation and anion in the case of optical phonons. However, as we will show below, there always exists a simple linear relationship between cation and anion displacements. It allows the restriction to one atomic displacement field, which satisfies the connection rules (3) and (4) for all phonons in GaAs-AlAs superlattices. However, it is noteworthy that the boundary conditions (3) and (4) are not generally valid. They reflect strongly the particular geometrical and chemical interface structures and depend also on the choice of the dynamical matrix.

III. SOLUTIONS

A. Mechanical modes

The equations of motion for the cations and anions in the general form (1) represent inhomogeneous differential equations with a complicated differential operator with respect to the coordinate z, even for phonons from the center of the Brillouin zone. However, since the fields (2) on the right-hand sides are themselves functions of the displacement fields, it is possible to discuss two different types of solutions, in agreement with the dispersionless limit.[34,35]

The first type of solution is characterized by the vanishing of the right-hand sides of Eqs. (1), i.e.,

$$E_{jy}(\theta)=D_{jz}(\theta)=0 . \tag{5}$$

These conditions are automatically satisfied for s-polarized phonons related to vibrations only in x direction, for p-polarized antisymmetrical phonons for which the resulting dipole moment of a superlattice elementary cell vanishes, and for p-polarized symmetrical phonons propagating parallel to the superlattice axis, i.e., $\theta=0$. Since the excitation of these modes is not accompanied by a y component of the electric field and a z component of the dielectric displacement field, we will call them *mechanical modes* in contrast to the *Coulomb modes*[36] usually related to such fields, at least if the bulk-phonon-branch dispersion is not neglected.

As a consequence of the zero field components on the right-hand sides of Eqs. (1) the Cartesian displacement directions are completely decoupled for the mechanical modes. Obviously, in each material layer the resulting displacement fields $u_{\alpha/j\alpha}(z,\theta)$ for cations and anions can

be expanded in terms of linearly independent exponential functions

$$\exp[\lambda_{\ell j\alpha}(\theta)z], \quad \exp[-\lambda_{\ell j\alpha}(\theta)z]$$

with a complex decay constant $\lambda_{\ell j\alpha}(\theta)$.[40] Then the frequencies of the eigenmodes can be represented by the expression

$$\omega_j^2(\theta)=\frac{\omega_{\ell\alpha}^2}{2}\left\{1\pm\left[1+\frac{4M_{1\ell}M_{2\ell}}{(M_{1\ell}+M_{2\ell})^2}\times\sinh^2\left[\lambda_{\ell j\alpha}(\theta)\frac{a_0}{4}\right]\right]^{1/2}\right\}, \tag{6}$$

where the zone-center optical frequencies

$$\omega_{\ell x}=\omega_{\ell y}=\omega_{\mathrm{TO}\ell}(\Gamma)=\left[f_\ell\left(\frac{1}{M_{1\ell}}+\frac{1}{M_{2\ell}}\right)\right]^{1/2},$$
$$\omega_{\ell z}=\omega_{\mathrm{LO}\ell}(\Gamma)=\left[(f_\ell+\hat{f})\left(\frac{1}{M_{1\ell}}+\frac{1}{M_{2\ell}}\right)\right]^{1/2} \tag{7}$$

of the underlying bulk zinc-blende-structure materials are introduced. Since for the vanishing right-hand sides in Eqs. (1) the different vibration directions are decoupled, the index of the Cartesian component α as well as the sign in expression (6) enter the characterization of phonon branches j in the center of the superlattice Brillouin zone. As an eigenvalue of a Hermitian problem, $\omega_j^2(\theta)$ must be a real number; hence, the decay constant $\lambda_{\ell j\alpha}(\theta)$ must be purely real or imaginary or complex with a constant imaginary part $\mathrm{Im}\lambda_{\ell j\alpha}(\theta)=2\pi/a_0$, indicating that evanescent or propagating waves can occur in a certain material layer. We mention that for pure imaginary decay constants $\lambda_{\ell j\alpha}(\theta)=ik_{\ell j\alpha}(\theta)$ and $-2\pi/a_0<k_{\ell j\alpha}<2\pi/a_0$ expression (6) describes the dispersion relations of the bulk optical (+) or acoustic (−) phonons along the ΓX high-symmetry line in the fcc Brillouin zone.[30]

In general, the branch frequencies $\omega_j(\theta)$, Eq. (6), have to be independent of the particular material. Such a requirement generates conditions for the decay constants $\lambda_{\ell j\alpha}(\theta)$ in different material layers ℓ and a possible classification of long-wavelength phonons in superlattices. The allowed energy regions for the bulk-phonon branches are characterized by the frequencies of the zone-center phonons (7) and those of the phonons at the X point of the Brillouin zone,

$$\Omega_{\ell x}=\Omega_{\ell y}=\omega_{\mathrm{TO}\ell}(X)=\left[f_\ell\frac{1}{M_{1\ell}}\right]^{1/2},$$
$$\Omega_{\ell z}=\omega_{\mathrm{LO}\ell}(X)=\left[(f_\ell+\hat{f})\frac{1}{M_{1\ell}}\right]^{1/2},$$
$$\hat{\Omega}_{\ell x}=\hat{\Omega}_{\ell y}=\omega_{\mathrm{TA}\ell}(X)=\left[f_\ell\frac{1}{M_{2\ell}}\right]^{1/2}, \tag{8}$$
$$\hat{\Omega}_{\ell z}=\omega_{\mathrm{LA}\ell}(X)=\left[(f_\ell+\hat{f})\frac{1}{M_{2\ell}}\right]^{1/2}.$$

Outside the energy regions, $0\le\omega_j(\theta)\le\hat{\Omega}_{\ell\alpha}$ and $\Omega_{\ell\alpha}\le\omega_j(\theta)\le\omega_{\ell\alpha}$, allowed in the bulk materials, the real part of the decay constant cannot vanish. More strictly, the corresponding phonon amplitude has to decay exponentially normal to the interfaces into the material ℓ. On the other hand, if the frequency $\omega_j(\theta)$ is within a region that is already allowed in the bulk, the corresponding decay constant can be purely imaginary. The resulting displacement field represents propagating waves or, more strictly, because of the layered structure (counterpropagating) standing waves in this material.

In the case of the material combination GaAs-AlAs the optical-phonon branches are energetically well separated. For that reason the AlAs-like (GaAs-like) optical phonons in such a system with $\Omega_{2\alpha}<\omega_j(\theta)<\omega_{2\alpha}$ [$\Omega_{1\alpha}<\omega_j(\theta)<\omega_{1\alpha}$] should be related to an imaginary decay constant $\lambda_{2j\alpha}(\theta)$ [$\lambda_{1j\alpha}(\theta)$] in the corresponding material, whereas $\lambda_{1j\alpha}(\theta)$ [$\lambda_{2j\alpha}(\theta)$] has a nonvanishing real part with an appropriate sign. This mechanical type of optical phonon is always confined[31,33] to one material. On the other hand, the energy regions of acoustic phonons of GaAs and AlAs are strongly overlapping. That means that the corresponding decay constants $\lambda_{1j\alpha}(\theta)$ and $\lambda_{2j\alpha}(\theta)$ can be imaginary for both materials. As the strongest effect of the superlattice on the vibronic structure, we expect the folding[10,31,32] of the bulk acoustic-phonon branches from the fcc Brillouin zone to that of the tetragonal superlattice in the growth direction.

The validity of expression (6) for the eigenfrequencies of the zone-center phonons is connected to a linear relationship between the displacements of cations and anions within one material layer. Applying the ansatz of exponential functions, it follows from Eqs. (1) that

$$u_{1\ell j\alpha}(z,\theta)=\mp\Phi_{\ell\alpha}(\omega_j(\theta))u_{2\ell j\alpha}(z,\theta), \tag{9}$$

with the complex function

$$\Phi_{\ell\alpha}(\omega)=\left[\frac{\omega^2-\hat{\Omega}_{\ell\alpha}^2}{\omega^2-\Omega_{\ell\alpha}^2}\frac{\Omega_{\ell\alpha}^2}{\hat{\Omega}_{\ell\alpha}^2}\right]^{1/2}. \tag{10}$$

The anion displacements themselves can be combined from the exponential functions according to the symmetry of the modes under consideration. For the antisymmetrical vibrations one finds ($0\le z<d$)

$$u_{2\ell j\alpha}(z,\theta)=u_{\ell j\alpha}^{(-)}(\theta)\frac{\sinh[\lambda_{\ell j\alpha}(\theta)(z-d_1\delta_{\ell 2}-d_\ell/2)]}{\sinh(\lambda_{\ell j\alpha}(\theta)d_\ell/2)} \tag{11}$$

for the different polarization directions $\alpha=x$ (s polarization), $\alpha=y,z$ (p polarization), and arbitrary propagation direction θ. Symmetrical vibrations with s polarization ($\alpha=x$; arbitrary propagation direction, i.e., $0\le\theta\le\pi/2$)

or p polarization ($\alpha=y,z$; propagation parallel to the growth direction, i.e., $\theta=0$) can be described by

$$u_{2\ell j\alpha}(z,\theta)=u^{(+)}_{\ell j\alpha}(\theta)\frac{\cosh[\lambda_{\ell j\alpha}(\theta)(z-d_1\delta_{\ell 2}-d_\ell/2)]}{\cosh(\lambda_{\ell j\alpha}(\theta)d_\ell/2)} . \tag{12}$$

The determination of the decay constants $\lambda_{bj\alpha}(\theta)$ and, as a consequence, that of the frequencies $\omega_j(\theta)$ by means of Eq. (6) requires the application of the boundary conditions (3) and (4). Using the linear relation (9) they can be rewritten only to anion displacements. With their particular forms (11) and (12) one obtains, for the amplitudes

$$u^{(\pm)}_{1j\alpha}(\theta)=\pm u^{(\pm)}_{2j\alpha}(\theta) , \tag{13}$$

$$M_{21}[\omega_j^2(\theta)-\hat{\Omega}^2_{1\alpha}]\tanh\left[\frac{a_0}{4}\lambda_{1j\alpha}(\theta)\right]\begin{Bmatrix}\tanh(\lambda_{1j\alpha}(\theta)d_1/2)\\ \coth(\lambda_{1j\alpha}(\theta)d_1/2)\end{Bmatrix}u^{(\pm)}_{1j\alpha}(\theta)$$

$$=\mp M_{22}[\omega_j^2(\theta)-\hat{\Omega}^2_{2\alpha}]\tanh\left[\frac{a_0}{4}\lambda_{2j\alpha}(\theta)\right]\begin{Bmatrix}\tanh(\lambda_{2j\alpha}(\theta)d_2/2)\\ \coth(\lambda_{2j\alpha}(\theta)d_2/2)\end{Bmatrix}u^{(\pm)}_{2j\alpha}(\theta) , \tag{13'}$$

where in our particular case $M_{21}=M_{22}$ corresponds to the mass of an arsenic atom. The system of homogeneous equations (13) for the amplitudes of the displacements in the two different materials can be solved by the ansatz

$$u^{(\pm)}_{\ell j\alpha}(\theta)=(\mp 1)^\ell D^{(\pm)}_{\ell j\alpha}(\theta)C^{(\pm)}_{j\alpha}(\theta) , \tag{14}$$

with the material-independent normalization constant $C^{(\pm)}_{j\alpha}(\theta)$ and the complex function

$$D^{(\pm)}_{\ell j\alpha}(\theta)=\frac{\coth\left[\frac{a_0}{4}\lambda_{\ell j\alpha}(\theta)\right]}{1-\hat{\Omega}^2_{\ell\alpha}/\omega_j^2(\theta)}\begin{Bmatrix}\coth(\lambda_{\ell j\alpha}(\theta)d_\ell/2)\\ \tanh(\lambda_{\ell j\alpha}(\theta)d_\ell/2).\end{Bmatrix} \tag{15}$$

The solubility condition of the system (13) then reads ($\alpha=x,y$ or z)

$$D^{(\pm)}_{j\alpha}(\theta)=\sum_{\ell=1}^{2} D^{(\pm)}_{\ell j\alpha}(\theta)=0 . \tag{16}$$

By means of the two equations (6) valid for $\ell=1$ and $\ell=2$ and the condition (16) the frequency $\omega_j(\theta)$ and the two decay constants $\lambda_{1j\alpha}(\theta)$, $\lambda_{2j\alpha}(\theta)$ can now be determined for each phonon mode j,θ at the center of the superlattice Brillouin zone.

B. Coulomb modes

With inclusion of the bulk-phonon-branch dispersion, the long-range electric fields $E_{jy}(\theta)$ and $D_{jz}(\theta)$ are generally different from zero for all symmetrical p-polarized ($\alpha=y,z$) phonons not propagating parallel to the superlattice axis ($\theta=0$), in contrast to the dispersionless case.[28,30,37,38] Due to the structure of Eqs. (1) for these vibrations, the general solutions are sums of two different contributions,

$$u_{\alpha\ell j\alpha}(z,\theta)=u^{(H)}_{\alpha\ell j\alpha}(z,\theta)+u^{(I)}_{\alpha\ell j\alpha}(z,\theta) . \tag{17}$$

The first contribution $u^{(H)}_{\alpha\ell j\alpha}(z,\theta)$ fulfills the system of "homogeneous" equations. They are therefore defined by Eqs. (9) and (12). The second contributions represent particular solutions of the system of "inhomogeneous" equations. They should be constants with respect to z. They can be formally written in the form

$$u^{(I)}_{1\ell j\alpha}(z,\theta)=-\frac{M_{2\ell}}{M_{1\ell}}u^{(I)}_{2\ell j\alpha}(z,\theta) , \tag{18}$$

$$u^{(I)}_{2\ell j\alpha}(z,\theta)=\frac{e^*}{M_{2\ell}}\frac{E_{jy}(\theta)\delta_{\alpha y}+D_{jz}(\theta)\delta_{\alpha z}}{\omega_j^2(\theta)-\omega^2_{\ell\alpha}} , \tag{19}$$

where the field components $E_{jy}(\theta)$ and $D_{jz}(\theta)$ are, however, related to the total displacements (17).

The complete solutions (17) again have to satisfy the continuity conditions (3) and (4). Applying relations (9), (12), (18), and (19) and $M_{21}=M_{22}=M_2$, one can show that Eq. (4) is automatically satisfied because constant contributions (18) and (19) are not affected by the differential operator in Eq. (4). With this particular form of the homogeneous part of the amplitude (14) and the definition (16) of $D^{(+)}_{j\alpha}(\theta)$, it follows from Eq. (3)

$$D^{(+)}_{j\alpha}(\theta)C^{(+)}_{j\alpha}(\theta)=\frac{e^*}{M_2}[E_{jy}(\theta)\delta_{\alpha y}+D_{jz}(\theta)\delta_{\alpha z}]\left[\frac{1}{\omega_j^2(\theta)-\omega^2_{1\alpha}}-\frac{1}{\omega_j^2(\theta)-\omega^2_{2\alpha}}\right] . \tag{20}$$

This relation allows the introduction of a normalization constant $C_{j\alpha}(\theta)$ of the full displacement field (17)

$$C_{j\alpha}(\theta)=\frac{e^*}{M_2}\frac{E_{jy}(\theta)\delta_{\alpha y}+D_{jz}(\theta)\delta_{\alpha z}}{D^{(+)}_{j\alpha}(\theta)}=C^{(+)}_{j\alpha}(\theta)\frac{[\omega_j^2(\theta)-\omega^2_{1\alpha}][\omega_j^2(\theta)-\omega^2_{2\alpha}]}{\omega^2_{1\alpha}-\omega^2_{2\alpha}} . \tag{21}$$

By means of the constant (21) the complete solutions of the equations of motion (1) for p-polarized phonons that satisfy the boundary conditions (3) and (4) take a concrete form. One gets for the anion envelope functions ($\alpha=y,z$)

$$u_{2\ell j\alpha}(z,\theta)=C_{j\alpha}(\theta)\left[(-1)^{\ell}\left[\frac{1}{\omega_j^2(\theta)-\omega_{1\alpha}^2}-\frac{1}{\omega_j^2(\theta)-\omega_{2\alpha}^2}\right]D_{\ell j\alpha}^{(+)}(\theta)\frac{\cosh[\lambda_{\ell j\alpha}(\theta)(z-d_1\delta_{\ell 2}-d_\ell/2)]}{\cosh(\lambda_{\ell j\alpha}(\theta)d_\ell/2)}+\frac{D_{j\alpha}^{(+)}(\theta)}{\omega_j^2(\theta)-\omega_{\ell\alpha}^2}\right]. \tag{22}$$

The cation envelope functions can be directly derived putting expression (22) in the equations of motion (1). We get ($\alpha=y,z$)

$$u_{1\ell j\alpha}(z,\theta)=-C_{j\alpha}(\theta)\left[(-1)^{\ell}\Phi_{\ell\alpha}(\omega_j(\theta))\left[\frac{1}{\omega_j^2(\theta)-\omega_{1\alpha}^2}-\frac{1}{\omega_j^2(\theta)-\omega_{2\alpha}^2}\right]D_{\ell j\alpha}^{(+)}(\theta)\times\frac{\cosh[\lambda_{\ell j\alpha}(\theta)(z-d_1\delta_{\ell 2}-d_\ell/2)]}{\cosh(\lambda_{\ell j\alpha}(\theta)d_\ell/2)}+\frac{M_{2\ell}}{M_{1\ell}}\frac{D_{j\alpha}^{(+)}(\theta)}{\omega_j^2(\theta)-\omega_{\ell\alpha}^2}\right]. \tag{23}$$

We mention that expressions (22) and (23) are straightforward generalizations of the very recent findings of a correct dispersionless macroscopic theory[33–35] for arbitrary decay constants $\lambda_{\ell j\alpha}(\theta)$.

The normalization constants $C_{j\alpha}(\theta)$ ($\alpha=y,z$) are coupled by Eqs. (2) defining the long-range electric-field components $E_{jy}(\theta)$ and $D_{jz}(\theta)$. Applying these definitions and the relation (21) one has to solve the system of equations

$$\begin{bmatrix}[\epsilon_y(\omega_j(\theta))D_{jy}^{(+)}(\theta)+W_y(\omega_j(\theta))]\sin\theta & D_{jz}^{(+)}(\theta)\cos\theta\\ D_{jy}^{(+)}(\theta)\cos\theta & -[\epsilon_z(\omega_j(\theta))D_{jz}^{(+)}(\theta)-W_z(\omega_j(\theta))]\sin\theta\end{bmatrix}\begin{bmatrix}C_{jy}(\theta)\\ C_{jz}(\theta)\end{bmatrix}=\begin{bmatrix}0\\0\end{bmatrix}, \tag{24}$$

where the dimensionless quantities

$$W_\alpha(\omega)=\frac{1}{N_1+N_2}\frac{\hat{f}}{M_2}\omega^2\left[\frac{1}{\omega^2-\omega_{1\alpha}^2}-\frac{1}{\omega^2-\omega_{2\alpha}^2}\right]^2 \tag{25}$$

and ($\alpha,\alpha'=y,z;\alpha\neq\alpha'$)

$$\epsilon_\alpha(\omega)=\sum_{\ell=1}^{2}\frac{N_\ell}{N_1+N_2}\frac{\omega^2-\omega_{\ell\alpha'}^2}{\omega^2-\omega_{\ell\alpha}^2} \tag{26}$$

are introduced. The first quantities (25) connect the bulk LO-TO splitting and the bulk-phonon-branch dispersion (in particular, indicated by the appearance of M_2) with the extent of the superlattice period $d=(N_1+N_2)a_0/2$. The second quantities (26) characterize the space-averaged dielectric function ($\alpha=y$) and, respectively, inverse dielectric function ($\alpha=z$) of the superlattice ignoring the background electronic polarization.[29,34]

The solubility condition of the system of equations (24) gives rise to an implicit angle-dependent dispersion relation for the eigenfrequencies $\omega_j(\theta)$ of the $2(N_1+N_2)$ symmetrical p-polarized superlattice phonon modes,

$$[\epsilon_y(\omega_j(\theta))D_{jy}^{(+)}(\theta)+W_y(\omega_j(\theta))][\epsilon_z(\omega_j(\theta))D_{jz}^{(+)}(\theta)-W_z(\omega_j(\theta))]\sin^2\theta+D_{jy}^{(+)}(\theta)D_{jz}^{(+)}(\theta)\cos^2\theta=0\ . \tag{27}$$

This relation is evidently a remarkable generalization of the result from the dispersionless limit.[29,34] Particularly, it describes a coupling of the confined optical phonons and the polar interface modes of the Fuchs-Kliewer type due to the appearance of the terms $W_\alpha(\omega)$ (25) in Eq. (27). These p-polarized phonons are intermixed according to the fact that the bulk-phonon-branch dispersion is taken into account. Thereby, the strong anisotropy with θ of the interface modes of the dispersionless limit are distributed among all Coulomb modes.

As an example the solutions of Eq. (27) for three different Coulomb modes LO1, LO3, and TO1 and the attached anion displacement patterns according to Eq. (22) of the envelope-function theory are shown in Fig. 1. We observe complete agreement of the envelope-function theory with the microscopic one. The envelopes completely describe the real atomic displacements due to the inclusion of the bulk-phonon-branch dispersion. Even in the case of Coulomb modes the strong changes of the pattern behavior, especially with respect to the number of nodes and the polarization direction, with the phonon propagation direction θ are reflected. We note that the transition of the polarization direction $z(y)$ for $\theta=0$ to $y(z)$ for $\theta=\pi/2$ for the LO3 (TO1) mode strongly indicates the intermixing of the confined and interface character of these two modes, as indicated by Eq. (27). The partial interface character of these nominally GaAs-like phonons for $\theta>0$ can also be seen from the small but finite atomic displacements in the AlAs region. Figure 1 also illustrates the problem of mode ordering in the

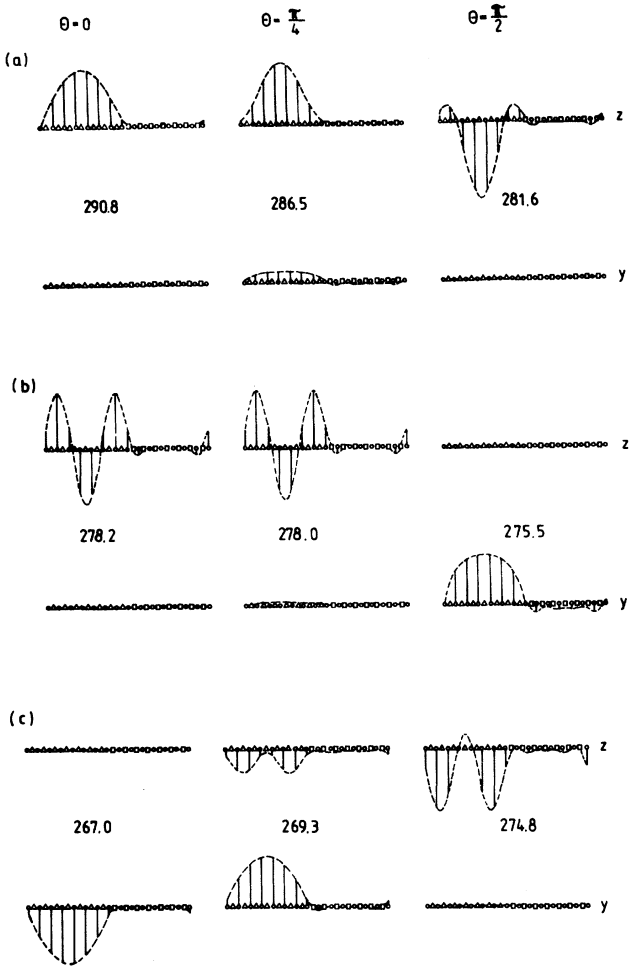

FIG. 1. Patterns of anion displacements in the z and y directions resulting from the microscopic theory (vertical solid lines) and according to the envelope-function theory (dashed lines) for the first three, (a)=LO1, (b)=LO3, (c)=TO1, symmetrical p-polarized GaAs-like modes. Parameters of a $(GaAs)_7(AlAs)_7$ superlattice are chosen. The numbers give the corresponding mode frequencies $\omega_j(\theta)$ (in units of cm^{-1}) for three propagation direction angles θ. Atomic positions are indicated by circles (arsenic), triangles (gallium), and squares (aluminum).

dependence on the phonon propagation direction θ. Similarly to the dispersionless case[33–35] we observe that with rising θ the LO1 mode goes down in energy and becomes a three-node mode. For $\theta=\pi/2$ LO1 looks like the LO3 mode at $\theta=0$. Simultaneously the non-Coulombic mode LO2, which shows no angle dispersion, appears as the highest-energy mode at $\theta=\pi/2$. These findings are in complete agreement with those of Huang and Zhu.[33] Only, their interpretation that the LO1 mode for $\theta=0$ becomes a Fuchs-Kliewer interface mode for $\theta>0$ is not correct considering the angle dispersion of LO1 and the above discussion of the interface character of calculated modes.

For the same parameters as in Fig. 1 the anion and cation envelope functions related to LO1 are compared in

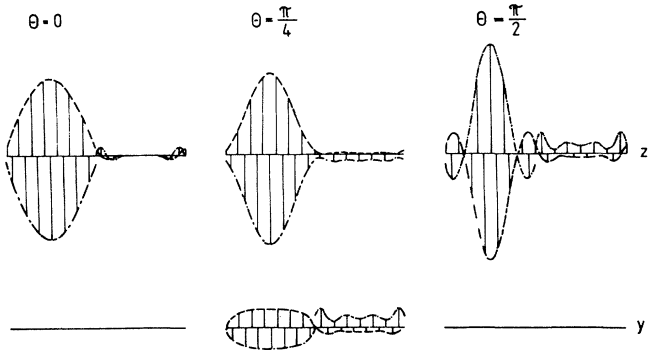

FIG. 2. Comparison of anion (dashed lines) and cation (dashed-dotted lines) displacement patterns in the z and y directions for the GaAs-like LO1 mode. Vertical solid lines indicate the atomic displacements resulting from the microscopic theory. The same parameters as in Fig. 1 are used.

Fig. 2 in more detail. This figure clearly demonstrates the different boundary conditions, the continuity of the anion displacement envelope, and, respectively, the near continuity of the derivative of the cation displacement envelope. Both displacement patterns show the decreasing confined character of the LO1 mode with rising propagation angle θ typically for Coulomb modes. Applying the cation and anion displacements shown in Fig. 2 the dipole moment of the LO1 mode can be constructed. Since zero y components, for $\theta=0$ and $\theta=\pi/2$ the variation of this polarization field versus z describes the shape of the z component of the electric field. The accompanying electrostatic potential shows a reverse symmetry, in complete agreement with studies[33,34] of the dispersionless limit, at least for phonon propagation nearly parallel to the interfaces. The dispersion does not change the symmetry of the potential. Moreover, the potential is continuous at the interfaces, even if the cation displacement jumps.

IV. LIMITING CASES OF SOLUTIONS

A. On the validity of the macroscopic theory

The strongest effect of the inclusion of the full bulk-phonon-branch dispersion on the superlattice phonons with vanishing wave vector concerns the symmetrical p-polarized modes not propagating parallel to the growth direction—the so-called Coulomb modes. As can be seen from the implicit dispersion relation, Eq. (27), there is a strong anisotropy with the propagation angle θ and a coupling of nominal bulklike and interfacelike modes. This coupling is governed by the quantities $W_\alpha(\omega)$, Eq. (25). If the inequalities ($\alpha=y,z$)

$$|\epsilon_\alpha(\omega)D_{j\alpha}^{(+)}(\theta)| \gg |W_\alpha(\omega)| \tag{28}$$

are fulfilled, relation (27) can be written as a product. The vanishing of each factor for $\omega=\omega_j(\theta)$ can satisfy this relation, more strictly,

$$D_{jy}^{(+)}(\theta)=0 \quad \text{or} \quad D_{jz}^{(+)}(\theta)=0 , \tag{29}$$

or

$$\epsilon_y(\omega)\epsilon_z(\omega)\sin^2\theta+\cos^2\theta=0 \ . \tag{30}$$

The first equations (29) practically give rise to the same angle-independent solutions as those given in Eq. (16) for the pure mechanical modes. The second relation (30) corresponds to the implicit dispersion relation for the Fuchs-Kliewer interface modes in the optical region.[17,20,23,29,34]

The quantities $W_\alpha(\omega)$ in Eq. (25) define the strength of coupling between mechanical and polar interface modes in the symmetrical p-polarized case. They depend on the thicknesses of material layers, the polar coupling (LO-TO splitting) in the underlying semiconductors and the approach of the eigenfrequencies to the bulk optical zone-center frequencies $\omega_{\ell y}=\omega_{\mathrm{TO}\ell}(\Gamma)$ or $\omega_{\ell z}=\omega_{\mathrm{LO}\ell}(\Gamma)$, Eq. (7). Due to the divergent character of the functions (25) for frequencies ω near the zone-center frequencies $\omega_{\ell\alpha}$ the inequality (28) (and thereby the macroscopic dispersionless theory) is nearly valid for eigenvalues far from the bulk LO or TO frequencies from the center of the Brillouin zone. Applying Eq. (28) for eigenfrequencies from the optical region, $\omega_j^2(\theta)=\omega_{\ell\alpha}^2+\Delta\omega_j^2(\theta)$, one finds the rough estimate

$$\Delta\omega_j^2(\theta)\gg\frac{1}{N_\ell}\frac{1}{1+\dfrac{M_2}{M_{1\ell}}}\omega_{\ell\alpha}^2 \ . \tag{31}$$

That means, even for the confined optical solutions of the dispersionless macroscopic theory[16,17,19–21,23,24] with frequencies $\omega_j^2(\theta)=\omega_{\ell\alpha}^2$, the neglect of the bulk-phonon-branch dispersion defined by $\hat{f}$ and M_2 is not valid. On the other hand, the rough estimate in Eq. (31) shows that for superlattices with very thick material layers, $d_\ell=N_\ell a_0/2$, the dispersionless macroscopic theory gives reasonable results even for frequencies $\omega_j^2(\theta)\lesssim\omega_{\ell\alpha}^2$.

B. Dispersionless limit for optical phonons

The dispersion of the bulk optical-phonon branches along the ΓX line in the Brillouin zone vanishes for $\omega^2=\omega_{b\alpha}^2=\Omega_{\ell\alpha}^2$. This can be formally reached by setting $M_2\to\infty$ since the anion mass is more or less responsible for this dispersion.[34] In this limit the eigenvalues of the mechanical modes in the optical-frequency region of the material ℓ are given by ($\alpha=x,y,z$)

$$\omega_j^2(\theta)=\omega_{\ell\alpha}^2, \quad \lambda_{\ell j\alpha}(\theta)=ik_{\ell j\alpha}(\theta) \ , \tag{32}$$

the frequencies of the optical zone-center phonons and purely imaginary decay constants $\lambda_{\ell j\alpha}$ according to Eq. (6). For all other frequencies the real parts of the decay constants are infinite. With $\hat{\Omega}_{\ell\alpha}^2=0$ one gets from Eqs. (15) and (16)

$$D_{j\alpha}^{(\pm)}(\theta)=\frac{1}{\sin\left[k_{\ell j\alpha}(\theta)\dfrac{a_0}{4}\right]}\left\{\begin{array}{l}-\dfrac{\cos\left[k_{\ell j\alpha}(\theta)\left[d_\ell+\dfrac{a_0}{2}\right]\Big/2\right]}{\sin(k_{\ell j\alpha}(\theta)d_\ell/2)}\\ +\dfrac{\sin\left[k_{\ell j\alpha}(\theta)\left[d_\ell+\dfrac{a_0}{2}\right]\Big/2\right]}{\cos[k_{\ell j\alpha}(\theta)d_\ell/2]}\end{array}\right. \ . \tag{33}$$

For mechanical modes the functions $D_{j\alpha}^{(\pm)}(\theta)$, Eq. (33), have to be zero according to Eq. (16). Hence, confined optical phonons result with wave vectors

$$k_{\ell j\alpha}(\theta)=\frac{\pi n}{d_\ell+a_0/2}=\frac{2\pi}{a_0}\frac{n}{N_\ell+1} \tag{34}$$

(with n odd for symmetrical modes and n even for antisymmetrical modes) and the limitation $1\le n\le N_\ell$ according to the extent of the bulk Brillouin zone. The accompanying envelopes of the cation displacements, (11) and (12), represent pure standing waves. From the point of view of macroscopic theory, i.e., $a_0\to 0$, $N_\ell\to\infty$ but $d_\ell=$const, these mechanical modes vibrating with the frequency $\omega_{\ell\alpha}$ are completely confined within the material layer ℓ and the corresponding displacement patterns exhibit nodes at the interfaces.

In the case of Coulomb modes ($\alpha=y,z$) there also exist solutions corresponding to Eq. (32). However, the limit $M_2\to\infty$ has to be performed with more care due to the divergency of the factors $W_\alpha(\omega)$, Eq. (25), with respect to these frequencies. To be consistent with the boundary condition (20) one has to require that the long-range electric-field components $E_{jy}(\theta)$ and $D_{jz}(\theta)$ vanish as $\omega_j^2(\theta)-\omega_{\ell\alpha}^2$. More strictly speaking, they have to be zero, which gives rise to new conditions to the confinement wave vector $k_{\ell j\alpha}(\theta)$ in Eq. (32). The anion displacements are practically zero. With Eq. (23) the cation displacement patterns take the form ($\alpha=y,z$)

$$u_{1\ell j\alpha}(z,\theta)=\left[\frac{\hbar}{2M_{1\ell}\omega_j(\theta)(N_1+N_2)}\right]^{1/2}\left[\frac{2}{d_\ell}\right]^{1/2}\frac{\cos[k_{\ell j\alpha}(\theta)(z-d_1\delta_{\ell 2}-d_\ell/2)]-\cos\left[k_{\ell j\alpha}(\theta)\left[d_\ell+\dfrac{a_0}{2}\right]\Big/2\right]}{\sin(k_{\ell j\alpha}(\theta)d_\ell/2)} \ , \tag{35}$$

with confinement wave vectors $k_{\ell j\alpha}(\theta)$ that satisfy the transcendental equation

$$\tan\left[k_{\ell j\alpha}(\theta)\left[d_\ell+\frac{a_0}{2}\right]\Big/2\right] =(N_\ell+1)\tan\left[k_{\ell j\alpha}(\theta)\frac{a_0}{4}\right] . \quad (36)$$

The confinement wave vectors $k_{\ell j\alpha}(\theta)$ for the symmetrical p-polarized phonons propagating in a certain direction $\theta\neq 0$ differ remarkably from the corresponding values $2\pi n/[(N_\ell+1)a_0]$ for propagation parallel to the growth axis. The reason is related to the long-range electric-field components. For $\theta\neq 0$ they do not automatically vanish but only for particular wave vectors and certain constant shifts of the displacement patterns. A discontinuity results in the confinement wave vector $k_{\ell j\alpha}(\theta)$ of each p-polarized symmetrical optical-phonon mode going from $\theta=0$ to $\theta>0$. Mathematically it reflects the fact that the prefactors of $\sin^2\theta$ and $\cos^2\theta$ in the implicit dispersion relation Eq. (27) are of different order with respect to the anion mass. In the limit $M_2\to\infty$ it holds $[\epsilon_\alpha(\omega)D_{j\alpha}^{(+)}(\theta)\pm W_\alpha(\omega)]\sim M_2$. Hence, for any $\theta>0$ one obtains the implicit relation (36) for the confinement wave vector, whereas for θ exactly zero, Eq. (34) is valid. It is worthwhile mentioning that in the exact continuum approach, i.e., $a_0\to 0$, the relation (36) changes over into the same one proposed by Huang and Zhu[33] and the present authors[34,35]

$$\tan(k_{\ell j\alpha}(\theta)d_\ell/2)=k_{\ell j\alpha}(\theta)d_\ell/2 . \quad (36')$$

Thereby the statements of these papers concerning the correct solutions of the macroscopic equations are confirmed. For a detailed discussion of the resulting displacement patterns and the mode characters as well as a strict comparison with the microscopic theory the reader is referred to Refs. 33–35.

In the case of Coulomb modes there exists a second type of solution which is characterized by the implicit dispersion relation Eq. (30). Its eigenfrequencies vary within the intervals $\omega_{\ell y}<\omega_j(\theta)<\omega_{\ell z}$ ($\ell=1,2$), depending on the propagation angle θ. These modes represent the well-known macroscopic interface modes of the Fuchs-Kliewer type.[16,17,19–21,23,24,32] In the dispersionless limit, $M_2\to\infty$, and for phonons from the center of the superlattice Brillouin zone these solutions are characterized by zero displacements of anions and the vanishing of the "homogeneous" contribution to the envelope function (23) for the cations within the material layers. The explicit form of the constant cation displacement patterns is described in Ref. 34.

One question within the dispersionless theory concerns the assignment of one symmetrical, p-polarized AlAs-like and GaAs-like mechanical mode ($\theta=0$) to an interface mode for $\theta>0$. If an "infinite small" bulk-phonon dispersion and the limitation $n\le N_\ell$ of the modes are taken into account, one finds that the last occurring symmetrical LO mode and the first symmetrical TO mode should become interface phonons for $\theta>0$.

C. Effective thicknesses of material layers

Now we focus our attention on the modification of the results for optical phonons if the full bulk-phonon-branch dispersion is taken into account in an approximate manner. At first we particularly consider mechanical modes starting from the concept of effective layer thicknesses d_ℓ^* introduced by Sood *et al.*[3]

Mechanical superlattice phonons that vibrate with frequencies $\omega_j(\theta)$ in the optical region of the material ℓ can be represented nearly by a standing wave with wave number $k_{\ell j\alpha}(\theta)=\pi n/d_\ell$ in this material according to $\lambda_{\ell j\alpha}(\theta)=ik_{\ell j\alpha}(\theta)$. This standing wave decays exponentially with a decay constant $\lambda_{\ell' j\alpha}(\theta)$ into the neighboring layers filled with the material ℓ' ($\neq\ell$). In an effective sense such a displacement pattern can be replaced by that of a single standing wave confined to a material slab with the effective thickness

$$d_{\ell j\alpha}^*(\theta)=d_\ell+\frac{a_0}{2}X_{\ell j\alpha}(\theta) \quad (37)$$

and vanishing atomic displacements in the neighboring material ℓ'. Thereby, the effective thickness for each mechanical mode is defined by the requirement that the envelope functions (11) and (12) vanish at the boundaries of this effective material slab. This happens if the effective wave number is given by

$$k_{\ell j\alpha}(\theta)=\frac{\pi n}{d_{\ell j\alpha}^*(\theta)}=\frac{2\pi}{a_0}\frac{n}{N_\ell+X_{\ell j\alpha}(\theta)} . \quad (38)$$

As we recall in the case of vanishing dispersion [cf. Eq. (34)], $X_{\ell j\alpha}(\theta)=1$ holds; this is a value which is changed, depending on the strength of bulk phonon dispersion and the mode under consideration.

With the effective thicknesses and wave numbers in Eqs. (37) and (38), the functions $D_{j\alpha}^{(\pm)}(\theta)$, Eq. (16), can be written in a form similar to that given in Eq. (33):

$$D_{j\alpha}^{(\pm)}(\theta)=\frac{\omega_j^2(\theta)}{\omega_j^2(\theta)-\hat{\Omega}_{\ell\alpha}^2}\frac{1}{\sin\left[k_{\ell j\alpha}(\theta)\frac{a_0}{4}\right]}\left\{-\frac{\cos(k_{\ell j\alpha}(\theta)d_{\ell j\alpha}^*/2)}{\sin(k_{\ell j\alpha}(\theta)d_\ell/2)}+\frac{\sin(k_{\ell j\alpha}(\theta)d_{\ell j\alpha}^*/2)}{\cos(k_{\ell j\alpha}(\theta)d_\ell/2)}\right\} . \quad (39)$$

The ℓ-layer-like eigenmodes follow from the zeros of expression (39). One gets for the change of the material layer ℓ in units of a molecule-layer thickness $a_0/2, X_{\ell j\alpha}(\theta)$, the transcendental equation ($\ell \neq \ell'$)

$$\tan\left[X_{\ell j\alpha}(\theta)k_{\ell j\alpha}(\theta)\frac{a_0}{4}\right] = \frac{\omega_j^2(\theta)-\hat{\Omega}_{\ell\alpha}^2}{\omega_j^2(\theta)} D_{\ell' j\alpha}^{(\pm)}(\theta)\tan\left[k_{\ell j\alpha}(\theta)\frac{a_0}{4}\right], \quad (40)$$

where the complex functions $D_{\ell' j\alpha}^{(\pm)}(\theta)$ are defined in Eq. (15).

In the case of ℓ-layer-like optical phonons, Fig. 3 shows the shift $X_{\ell j\alpha}$, depending on the corresponding confinement wave number $k_{\ell j\alpha}$ for various thicknesses $N_{\ell'}$ of the neighboring material layers. For relatively small "barrier" thicknesses $N_{\ell'}$ of the order 3–5 the curves already approach the thick-layer limit, reflecting the fact of zero overlap of the displacement pattern tails from both interfaces. The effective thickness change $X_{\ell j\alpha}$ is in general a slowly varying function of the confinement wave number $k_{\ell j\alpha}$. Over a wide range of small $k_{\ell j\alpha}$, it is nearly a constant different from 1 and hence suitable for a characterization of the corresponding phonons. However, this is no longer valid for $k_{\ell j\alpha}$ near the boundary of the bulk Brillouin zone where $X_{\ell j\alpha}=1$. These results are able to give some insight into the different findings of Raman scattering on GaAs-AlAs superlattices[3,41] and bulk neutron-scattering data[42] for the bulk-optical-phonon-branch dispersion along the ΓX line.

For AlAs-like phonons one obtains the value $X_{\ell j\alpha} > 1$ from Fig. 3 according to the fact that the AlAs-like optical branches lie energetically above the GaAs-like ones. For GaAs-like modes the shift is generally smaller due to the stronger coupling to acoustic-phonon branches. We find $X_{\ell j\alpha} \approx 0.5$ for not too large confinement wave numbers. These values are in a rough agreement with other theoretical or experimental findings: $X_{\ell j\alpha}=0$ for GaAs,[3] $X_{\ell j\alpha}=1$ for GaAs,[5,9,41] $X_{\ell j\alpha}=1$ for AlAs,[10] and $X_{\ell j\alpha}=0.5$ for GaAs and AlAs.[28,30] To understand the reason for the discrepancies in more detail we consider the limit of thick neighboring layers, $N_{\ell'} \to \infty$. With $\hat{\Omega}_{1\alpha}=\hat{\Omega}_{2\alpha}$ one gets for confinement wave vectors near the zone center, i.e., $k_{\ell j\alpha}=0$, approximately from Eq. (40)

$$X_{\ell j} = \left[1 - \frac{M_{1\ell}^2}{M_2(M_{1\ell'}-M_{1\ell})+M_{1\ell}M_{1\ell'}}\right]^{-1/2}. \quad (41)$$

This approximate formula leads to $X_{\ell j}=1.08$ for AlAs-like modes and $X_{\ell j}=0.46$ for GaAs-like modes, in close agreement with the exact values in Fig. 3.

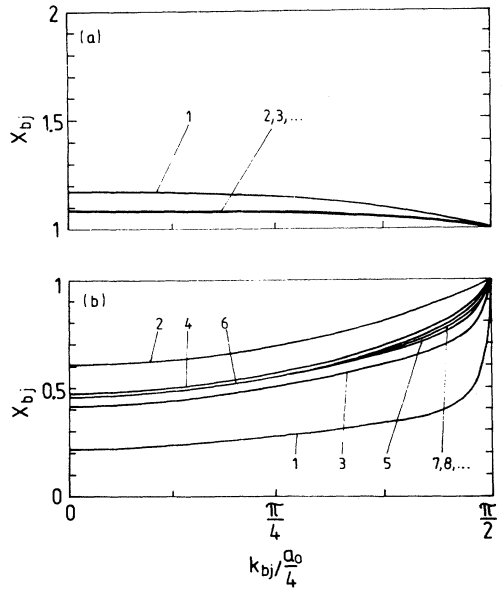

FIG. 3. Change of the effective thickness $X_{\ell j}$ vs the confinement wave number for several thicknesses $N_{\ell'}$, characterized by numbers 1,2,3, ... The upper part (a) shows the curves for AlAs-like modes; the lower part (b) characterizes GaAs-like modes for even $N_{\ell'}$.

D. Band-edge approximation for LOn Coulomb modes

Coulomb modes propagating in a certain direction θ are characterized by a coupling of different polarization directions, in our case, y and z [cf. Eq. (24)] and, therefore, by a coupling of nominal LO and TO bulk phonon branches of the corresponding material. In the case of such branches with weak dispersion and a relatively large energetic separation, which is nearly realized for AlAs, the dispersionless approach described in Sec. IV B yields more or less reasonable results, at least for the displacement patterns. In the case of stronger branch dispersion and an overlapping of both phonon bands, realized in GaAs, an approach, giving reasonable results for all modes, does not exist. One has to solve the full problem, Eq. (24), with realistic material parameters, the actual geometry of the superlattice (N_1,N_2), and the phonon propagation direction θ. On the other hand, detailed numerical studies[28,30] have shown that, for phonons with frequencies smaller than the zone-center TO frequency, the anisotropy of the corresponding modes is negligible compared with that of the symmetrical modes with $\omega_{\ell y} < \omega_j(\theta) < \omega_{\ell z}$. Therefore, we focus our attention on the anisotropic modes higher in energy than $\omega_{\ell y}$. More strictly, we only consider ℓ-layer-like symmetrical superlattice phonons with frequencies close to the band edge $\omega_{\ell z}$ of the LO bulk phonon bands of the corresponding material.

For modes with $\omega_{\ell y} < \omega_j(\theta) < \omega_{\ell z}$ the decay constant $\lambda_{\ell j\alpha}$ for the atomic displacements in the y direction is real. For this reason, the quantity $D_{jy}^{(+)}(\theta)$ in (15) is a slowly varying function with respect to the argument $\lambda_{\ell jy} d_\ell/2$. On the other hand, in the considered frequency region the other one $D_{jz}^{(+)}(\theta)$ in (15) is a strongly oscillating function for not-too-small layer thicknesses d_ℓ. Expanding all slowly varying terms in Eq. (27) one obtains ($\ell, \ell' = 1,2$; $\ell \neq \ell'$)

$$\tan(k_{\ell jz} d^*_{\ell jz}/2) = k_{\ell jz} d^*_{\ell jz} \Big/ 2 \left[1 - R_{\ell jz} \frac{(N_\ell + N_{\ell'})^2}{N_\ell^3 N_{\ell'}} \cot^2\theta (k_{\ell jz} d^*_{\ell jz}/2)^2 \right], \tag{42}$$

$$R_{\ell jz} = \frac{\omega^2_{\ell z} - \omega^2_{\ell' y}}{\omega^2_{\ell z} - \omega^2_{\ell' z}} \frac{\Omega^2_{\ell z} \hat{\Omega}^2_{\ell z}}{\omega^2_{\ell z}(\omega^2_{\ell z} - \omega^2_{\ell y})}, \tag{43}$$

a transcendental equation for $k_{\ell jz}$, which includes corrections in the lowest order with respect to $k_{\ell jz} a_0/4$ on the right-hand side. Besides the term proportional to the coefficient $R_{\ell jz}$, Eq. (43), the relation (42) has the same structure as the result of the macroscopic continuum theory, Eq. (36') in the dispersionless limit. However, the layer thicknesses d_ℓ are replaced by the effective ones $d^*_{\ell jz}$. The additional term $\sim\cot^2\theta$ clearly represents the anisotropy of the Coulomb modes. It smooths the discontinuity[34,35] in the mode behavior between $\theta=0$ and $\theta>0$ and vanishes for thick material layers N_ℓ. For increasing thickness $N_{\ell'}$, however, this term becomes infinite for all angles θ; that means, for double heterostructures, the anisotropy vanishes. The leading constant is $R_{\ell jz} = 1.03$ (1.47) for GaAs (AlAs). It vanishes in the dispersionless limit (formally $M_2 \to \infty$).

Relation (42) gives a qualitative insight into the angle dispersion of the first symmetrical LOn Coulomb modes (applying the nomenclature of the modes propagating parallel to the growth axis,[30]) with frequencies near the band edge $\omega_{\mathrm{LO}\ell}(\Gamma)$ of the corresponding bulk branch. To get an idea of the quantitative validity of the approximation made in deriving Eq. (42) we show the corresponding results for the angle dispersion of the confinement wave number $k_{\ell jz}$ and the eigenfrequency $\omega_j(\theta)$ in Figs. 4 and 5. The approximate results for eigenfrequencies are compared with the exact ones, given by Eq. (27). Figure 4 shows the expected smooth increase in the confinement wave vectors from $\theta=0$ to $\theta=\pi/2$, which is related to the change in the node structure of the displacement pattern. For the highest mode the approximation confirms the exact result that $n = k_{\ell j\alpha}(\theta) d^*_{\ell j\alpha}/\pi$ goes from $n=1$ ($\theta=0$) to $n \approx 3$ ($\theta=\pi/2$), as is known from the more extended studies.[33,34] With respect to the eigenfrequencies $\omega_j(\theta)$ excellent agreement of the approximation and the exact function is observed for the highest modes in Fig. 5. Discrepancies mainly concern propagation directions, with equal components parallel to the growth axis and the interfaces and modes with lower energies.

It is known that the strong transition region in the angle dispersions in Fig. 5 is related to the interface character of the modes in the intermediate-angle region. The interface character mixes the nominal LOn and TOn modes in the case $\theta=0$. As a result (cf. Fig. 5) the LO1 mode for $\theta=0$ carries the character of the LO3 mode at $\theta=\pi/2$. The interface character of these modes is related to appearance of atomic displacements in the y and z directions.

V. SUMMARY

We have described an analytical envelope-function theory for the long-wavelength phonon modes of a super-

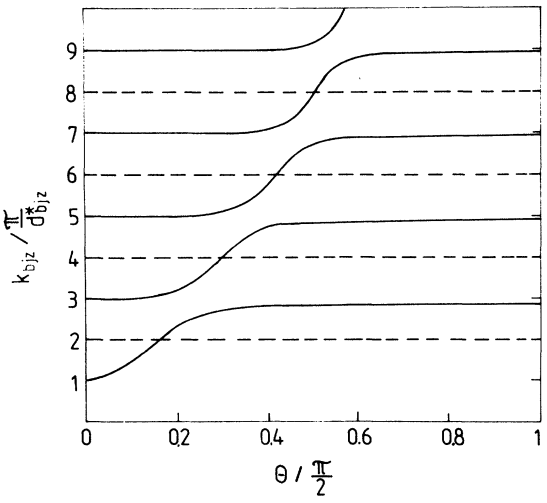

FIG. 4. Angle dispersion of the effective confinement wave number $k_{\ell jz}(\theta)$ according to Eq. (42) for the first symmetrical (solid lines) and antisymmetrical (dashed lines) GaAs-like LOn modes for a $(GaAs)_{25}(AlAs)_{25}$ superlattice.

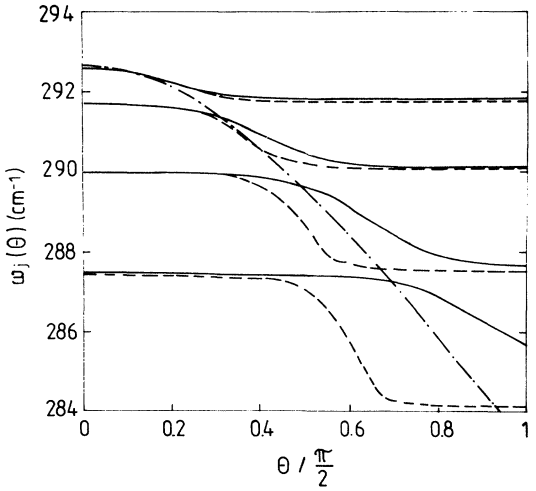

FIG. 5. Angle dispersion of the eigenfrequencies $\omega_j(\theta)$ of the first four symmetrical GaAs-like LOn modes for a $(GaAs)_{25}(AlAs)_{25}$ superlattice. Solid lines represent the exact results according to Eq. (27), whereas the dashed lines follow from the approximation in Eq. (42). For the purpose of comparison the dispersion of the upper GaAs-like interface phonon is shown as a dashed-dotted line.

lattice formed by polar semiconductors. Thereby, in the framework of simplified elastic forces in the lattice under consideration the full bulk-phonon-branch dispersion of the constituent materials is taken into account. We have shown that both the tangential component, $E_{jy}(\theta)$, of the electric field and the longitudinal component, $D_{jz}(\theta)$, of the electric displacement field introduced automatically satisfy the boundary conditions of macroscopic electrodynamics. The additional mechanical boundary conditions, necessary because of the inclusion of the full dispersion, are completely derived from the microscopic equations of motion.

The exact solution of the vibrational eigenvalue problem enforces a natural division into mechanical or Coulomb modes according to the vanishing or nonvanishing of the long-range electric-field components $E_{jy}(\theta)$ and $D_{jz}(\theta)$. The theory presented explains the relation of the mode spectrum and the displacement patterns of cations and anions in the two material layers, as well as reasons for anisotropy and polarization direction coupling of the Coulomb modes, which generally are mixtures of confined modes and interface phonons discussed in any dispersionless theory.

The envelope-function theory presented yields much insight into the validity and the correct solutions of the dispersionless macroscopic theory. Introducing the concept of effective layer thicknesses and considering Coulomb modes of the LOn type separately, we succeeded in deriving approximate expressions for eigenfrequencies and parameters of the envelope-function shapes which reflect the major dependences on material and geometry parameters in a correct manner. We gave approximate formulas which show clearly that for large material-layer thicknesses the dispersionless macroscopic theory can be a reasonable approach.

ACKNOWLEDGMENTS

One of the authors (H.G.) would like to express his deep gratitude to Humboldt University in Berlin for its kind hospitality in the course of this work. Helpful discussions with R. Enderlein, E. Molinari, P. Lugli, and E. Richter are gratefully acknowledged.

[1]J. E. Zucker, A. Pinczuk, D. S. Chemla, A. C. Gossard, and W. Wiegmann, Phys. Rev. Lett. **53**, 1280 (1984); Phys. Rev. B **29**, 7065 (1984).
[2]B. Jusserand, D. Paquet, J. Kervarec, and A. Regreny, J. Phys. (Paris) **45**, C5-145 (1984).
[3]A. K. Sood, J. Menendez, M. Cardona, and K. Ploog, Phys. Rev. Lett. **54**, 2111 (1985); **54**, 2115 (1985).
[4]B. Jusserand, D. Paquet, F. Alexandre, and A. Regreny, Surf. Sci. **174**, 94 (1986).
[5]B. Jusserand and D. Paquet, Phys. Rev. Lett. **56**, 1752 (1986).
[6]M. Nakayama, K. Kubota, H. Kato, and N. Sano, J. Appl. Phys. **60**, 3289 (1986).
[7]A. Ishibashi, Y. Mori, M. Itabashi, and N. Wathanabe, in *Proceedings of the 18th International Conference on the Physics of Semiconductors, Stockholm, 1986,* edited by O. Engstrom (World Scientific, Singapore, 1987).
[8]V. V. Gridin, R. Beserman, and H. Morkoç, Phys. Rev. B **37**, 9061 (1988).
[9]G. Fasol, M. Tanaka, H. Sakaki, and Y. Horikoshi, Phys. Rev. B **38**, 6056 (1988).
[10]Z. P. Wang, H. X. Han, G. H. Li, D. S. Jiang, and K. Ploog, Phys. Rev. B **38**, 8483 (1988).
[11]T. A. Gant, M. Delaney, M. V. Klein, R. Houdre, and H. Morkoç, Phys. Rev. B **39**, 1696 (1989).
[12]I. Sela, R. Beserman, and H. Morkoç, Phys. Rev. B **39**, 3254 (1989).
[13]A. Fasolino, E. Molinari, and J. C. Maan, Phys. Rev. B **39**, 3923 (1989).
[14]Z. V. Popović, M. Cardona, E. Richter, D. Strauch, and K. Ploog, Phys. Rev. B **40**, 1207 (1989).
[15]M. Born and K. Huang, *Dynamical Theory of Crystal Lattices* (Clarendon, Oxford, 1954).
[16]E. P. Pokatilov and S. I. Beril, Phys. Status Solidi B **118**, 567 (1983).
[17]V. M. Fomin and E. P. Pokatilov, Phys. Status Solidi B **132**, 69 (1985).
[18]C. Colvard, T. A. Gant, M. V. Klein, R. Merlin, R. Fischer, H. Morkoç, and A. C. Gossard, Phys. Rev. B **31**, 2080 (1985).
[19]R. Enderlein and F. Bechstedt, *Proceedings of the 18th International Conference on the Physics of Semiconductors, Stockholm, 1986* (Ref. 7).
[20]L. Wendler and R. Pechstedt, Phys. Status Solidi B **141**, 129 (1987).
[21]L. Wendler and R. Haupt, Phys. Status Solidi B **143**, 487 (1987).
[22]M. Babiker, J. Phys. C **19**, 683 (1986); Physica B+C **145**, 111 (1987).
[23]R. Enderlein, F. Bechstedt, and H. Gerecke, Phys. Status Solidi B **148**, 173 (1988).
[24]R. Enderlein, Phys. Status Solidi B **150**, 85 (1988).
[25]S.-K. Yip and Y.-C. Chang, Phys. Rev. B **30**, 7037 (1984).
[26]E. Richter and D. Strauch, Solid State Commun. **64**, 867 (1987).
[27]E. Molinari, A. Faslino, and K. Kunc, Superlatt. Microstruct. **2**, 397 (1986).
[28]S.-F. Ren, H. Chu, and Y.-C. Chang, Phys. Rev. Lett. **59**, 1841 (1987); Phys. Rev. B **37**, 8899 (1988).
[29]H. Chu, S.-F. Ren, and Y.-C. Chang, Phys. Rev. B **37**, 10 746 (1988).
[30]F. Bechstedt and H. Gerecke, Phys. Status Solidi B **154**, 565 (1989).
[31]M. Cardona, Superlatt. Microstruct. **5**, 27 (1989).
[32]M. V. Klein, IEEE J. Quantum Electron. **QE-22**, 1760 (1986).
[33]K. Huang and B.-F. Zhu, Phys. Rev. B **38**, 13 377 (1988).
[34]F. Bechstedt and H. Gerecke, Phys. Status Solidi B **156**, 151 (1989).
[35]F. Bechstedt and H. Gerecke, J. Phys. Condens. Matter **2**, 4363 (1990).
[36]B.-F. Zhu, Phys. Rev. B **38**, 7694 (1988).
[37]T. Tsuchiya, H. Akera, and T. Ando, Phys. Rev. B **39**, 6025 (1989).
[38]H. Akera and T. Ando, Phys. Rev. B **40**, 2914 (1989).
[39]See, e.g., L. D. Landau and E. M. Lifshitz, *Fluid Dynamics* (Pergamon, Oxford, 1963).

[40]Apart from the imaginary unit i, $\lambda_{\nearrow j\alpha}(\theta)$ represents a complex wave vector.

[41]B. H. Bairamov, R. A. Evarestov, I. P. Ipatova, Yu. E. Kitaev, A. Yu. Maslov, M. Delaney, T. A. Gant, M. V. Klein, D. Levi, J. Klem, and H. Morkoç, Superlatt. Microstruct. **6**, 227 (1989).

[42]cf. data given in Ref. 26.